RESEARCH ARTICLE

The Evolutionary Rewiring of Ubiquitination Targets Has Reprogrammed the Regulation of Carbon Assimilation in the Pathogenic Yeast *Candida albicans*

Doblin Sandai,* Zhikang Yin, Laura Selway, David Stead, Janet Walker, Michelle D. Leach,* Iryna Bohovych,* Iuliana V. Ene, Stavroula Kastora, Susan Budge, Carol A. Munro, Frank C. Odds, Neil A. R. Gow, and Alistair J. P. Brown

School of Medical Sciences, University of Aberdeen, Institute of Medical Sciences, Foresterhill, Aberdeen, United Kingdom

* Present address: Doblin Sandai, Institut Perubatan & Pergigian Termaju, Universiti Sains Malaysia, Pulau Pinang, Malaysia; Michelle D. Leach, Department of Molecular Genetics, University of Toronto, Toronto, Canada; Iryna Bohovych, Nebraska Redox Biology Center, University of Nebraska—Lincoln, Lincoln, Nebraska, USA

ABSTRACT **Microbes must assimilate carbon to grow and colonize their niches. Transcript profiling has suggested that *Candida albicans*, a major pathogen of humans, regulates its carbon assimilation in an analogous fashion to the model yeast *Saccharomyces cerevisiae*, repressing metabolic pathways required for the use of alterative nonpreferred carbon sources when sugars are available. However, we show that there is significant dislocation between the proteome and transcriptome in *C. albicans*. Glucose triggers the degradation of the *ICL1* and *PCK1* transcripts in *C. albicans*, yet isocitrate lyase (Icl1) and phosphoenolpyruvate carboxykinase (Pck1) are stable and are retained. Indeed, numerous enzymes required for the assimilation of carboxylic and fatty acids are not degraded in response to glucose. However, when expressed in *C. albicans*, *S. cerevisiae* Icl1 (ScIcl1) is subjected to glucose-accelerated degradation, indicating that like *S. cerevisiae*, this pathogen has the molecular apparatus required to execute ubiquitin-dependent catabolite inactivation. *C. albicans* Icl1 (CaIcl1) lacks analogous ubiquitination sites and is stable under these conditions, but the addition of a ubiquitination site programs glucose-accelerated degradation of CaIcl1. Also, catabolite inactivation is slowed in *C. albicans ubi4* cells. Ubiquitination sites are present in gluconeogenic and glyoxylate cycle enzymes from *S. cerevisiae* but absent from their *C. albicans* homologues. We conclude that evolutionary rewiring of ubiquitination targets has meant that following glucose exposure, *C. albicans* retains key metabolic functions, allowing it to continue to assimilate alternative carbon sources. This metabolic flexibility may be critical during infection, facilitating the rapid colonization of dynamic host niches containing complex arrays of nutrients.**

IMPORTANCE **Pathogenic microbes must assimilate a range of carbon sources to grow and colonize their hosts. Current views about carbon assimilation in the pathogenic yeast *Candida albicans* are strongly influenced by the *Saccharomyces cerevisiae* paradigm in which cells faced with choices of nutrients first use energetically favorable sugars, degrading enzymes required for the assimilation of less favorable alternative carbon sources. We show that this is not the case in *C. albicans* because there has been significant evolutionary rewiring of the molecular signals that promote enzyme degradation in response to glucose. As a result, this major pathogen of humans retains enzymes required for the utilization of physiologically relevant carbon sources such as lactic acid and fatty acids, allowing it to continue to use these host nutrients even when glucose is available. This phenomenon probably enhances efficient colonization of host niches where sugars are only transiently available.**

Received 5 November 2012 **Accepted** 13 November 2012 **Published** 11 December 2012

Citation Sandai D, et al. 2012. The evolutionary rewiring of ubiquitination targets has reprogrammed the regulation of carbon assimilation in the pathogenic yeast *Candida albicans*. mBio 3(6):e00495-12. doi:10.1128/mBio.00495-12.

Editor John W. Taylor, University of California

Address correspondence to Alistair J. P. Brown, al.brown@abdn.ac.uk.

Carbon assimilation is fundamentally important for all organisms. When faced with choices of carbon source, microbes often assimilate preferred carbon sources to support the first phase of growth and then, having exhausted these carbon sources, turn to alternative energetically less favorable carbon sources to drive subsequent phases of diauxic growth. This selective carbon utilization is reflected in the differential regulation of genes and enzymes that support the uptake and catabolism of specific carbon sources. The *Escherichia coli lac* operon provides a classic example of this, mediating lactose utilization only after the preferred carbon source, glucose, is exhausted (1, 2). In *Saccharomyces cerevisiae*, glucose limits the assimilation of alternative carbon sources and represses respiration under aerobic conditions, promoting fermentative metabolism (the Crabtree effect [3, 4]).

S. cerevisiae is exquisitely sensitive to sugars: even glucose concentrations as low as 0.01% trigger the major redirection of cellular resources (5, 6). Glucose exerts its dramatic effects upon *S. cerevisiae* physiology via signaling pathways that include the glucose repression (Snf1 AMP kinase) pathway, cyclic AMP (cAMP)-protein kinase A signaling, and the sugar receptor repressor (Snf3-Rgt2) pathway (for reviews, see references 7 to 12). The cAMP-protein kinase A pathway activates ribosome biogenesis

and downregulates stress responses in response to glucose (13–16). The sugar receptor repressor pathway modulates the expression of hexose transporters (9, 17, 18). Meanwhile, the glucose repression pathway represses the transcription of genes involved in the assimilation of alternative carbon sources, such as galactose, ethanol, and fatty acids (7, 8).

These sugar signaling mechanisms comprise an interlinked network rather than parallel signaling pathways (8, 10, 12, 18, 19). Furthermore, glucose regulation is imposed at multiple levels in *S. cerevisiae*. They include transcriptional (7–9), posttranscriptional (5, 6, 20, 21), translational (22), and posttranslational mechanisms (23–28). For example, glucose represses the transcription of genes encoding the gluconeogenic enzymes fructose 1,6-bisphosphatase (*FBP1*) and phosphoenolpyruvate carboxykinase (*PCK1*) (29, 30) and triggers the accelerated degradation of the *FBP1* and *PCK1* mRNAs (5, 20). Furthermore, glucose triggers the phosphorylation and inactivation of fructose 1,6-bisphosphatase (Fbp1) as well as its proteolytic degradation (31). The accelerated degradation of Fbp1 is mediated by vacuolar and ubiquitin-dependent mechanisms (28). Following glucose addition, Fbp1 is ubiquitinated and degraded via the proteasome (25, 28, 32). Like Fbp1, the glyoxylate cycle enzyme, isocitrate lyase (Icl1) is also subject to catabolite inactivation in *S. cerevisiae* (24). This tight control of central carbon metabolism is thought to reflect the evolution of this model yeast under conditions of "feast or famine" and to enhance the competitiveness of *S. cerevisiae* in sugar-rich niches containing complex microflora (9).

S. cerevisiae is often viewed as a paradigm for other yeasts (33). However, yeast species inhabit diverse niches and have evolved under contrasting selective pressures leading to differing strategies of carbon utilization (34). For example, the major systemic fungal pathogen of humans, *Candida albicans*, inhabits niches that contain complex mixtures of carbon sources. During commensalism and mucosal infection, *C. albicans* colonizes the oral cavity and the gastrointestinal and urogenital tracts, and during systemic infection, this pathogen can thrive in the bloodstream and most internal organs (35, 36). Few of these niches are rich in sugar. Blood glucose levels range from 4 to 7 mM (0.07 to 0.13%), whereas concentrations of about 111 mM (2%) are often used to impose glucose repression in *in vitro* experiments. Many niches are rich in alternative carbon sources, such as lactate, fatty acids, and amino acids. For example, lactic acid is found in ingested foods, is produced by host metabolic activity and by lactic acid bacteria in the gastrointestinal and urogenital tracts (37), and is essential for the proliferation of *Candida glabrata* in the intestinal tract (38). Also, glyoxylate cycle and fatty acid β-oxidation genes are expressed in the host and are required for the full virulence of *C. albicans* during systemic infections (39–42).

Although *C. albicans* occupies contrasting niches from *S. cerevisiae*, analogous sugar signaling pathways are thought to exist in these yeasts (33). Although there has been considerable rewiring of the regulatory circuitry that controls carbon metabolism (43–45), microarray experiments have revealed that *C. albicans* genes involved in the assimilation of alternative carbon sources are exquisitely sensitive to low concentrations of glucose (46, 47), like their orthologs in *S. cerevisiae* (6). However, unlike *S. cerevisiae*, *C. albicans* continues to respire in the presence of glucose, leading to its classification as a Crabtree-negative yeast (48).

These observations create an interesting conundrum relating to the carbon assimilation and pathogenicity of *C. albicans*: how can this yeast rapidly colonize niches that contain small amounts of glucose if many of the metabolic genes required for efficient growth in these niches are repressed by glucose? Could glucose regulation be relaxed at a posttranscriptional level in *C. albicans*, thereby facilitating simultaneous assimilation of sugars and alternative carbon sources *in vivo*? We have addressed these questions first by performing proteomic screens to identify proteins that are regulated in response to physiologically relevant carbon sources, revealing that gluconeogenic and glyoxylate cycle enzymes remain at high levels hours after glucose exposure. We then showed that *C. albicans* Pck1 and Icl1 are not destabilized by glucose, in contrast to *S. cerevisiae* Pck1 and Icl1, even though *C. albicans* has retained the molecular apparatus to program the accelerated, ubiquitin-mediated degradation of target proteins following glucose exposure. *C. albicans* Icl1 escapes degradation following glucose addition, because this enzyme lacks key ubiquitination sites required to target it for accelerated degradation. Our data show that there has been significant posttranscriptional rewiring during the evolution of this pathogen, thereby allowing *C. albicans* to continue to assimilate alternative carbon sources in the presence of glucose.

RESULTS

Carbon source has a major impact on the *C. albicans* proteome. Microarray studies have shown that the *C. albicans* transcriptome is exquisitely sensitive to glucose and that genes involved in the assimilation of alternative carbon sources are subject to glucose repression (46, 47). Our first aim was to establish whether this transcriptional regulation was reflected in the *C. albicans* proteome. To test this, we grew prototrophic *C. albicans* NGY152 cells (see Table S1 in the supplemental material) for 20 h in minimal medium containing glucose, lactate, oleate, or amino acids as the sole carbon source, harvested them in mid-exponential phase, prepared protein extracts, and subjected them to two-dimensional (2D) gel electrophoresis (Materials and Methods). Principal component analysis confirmed the reproducibility of the 2D gels from the independent replicate experiments and showed that the carbon source had a significant impact upon the *C. albicans* proteome (see Fig. S1A in the supplemental material). Proteins that displayed statistically significant changes in level on the basis of three independent experiments (Fig. 1A) were identified by tryptic digestion and matrix-assisted laser desorption ionization–time of flight (MALDI-ToF) mass spectrometry. Positive identifications were obtained for 206 2D gel features, representing 152 different *C. albicans* proteins, some distinct features representing isoforms of the same protein. The list of *C. albicans* proteins identified is presented in Table S2 and submitted to the PRIDE (proteomics identifications database) proteomic data repository (http://www.ebi.ac.uk/pride/) (accession numbers 3186 to 3192).

The network of proteins that displayed statistically significant changes in response to carbon source mainly comprised metabolic enzymes (Fig. 1B). Significant overlap was observed between the sets of proteins that were regulated in response to growth on lactate, oleate, or amino acids compared to the glucose condition. During growth on these organic acids, glycolytic enzymes were downregulated, and enzymes involved in gluconeogenesis, the glycoxylate cycle, the tricarboxylic acid (TCA) cycle and pathways involved in the assimilation of alternative carbon sources were

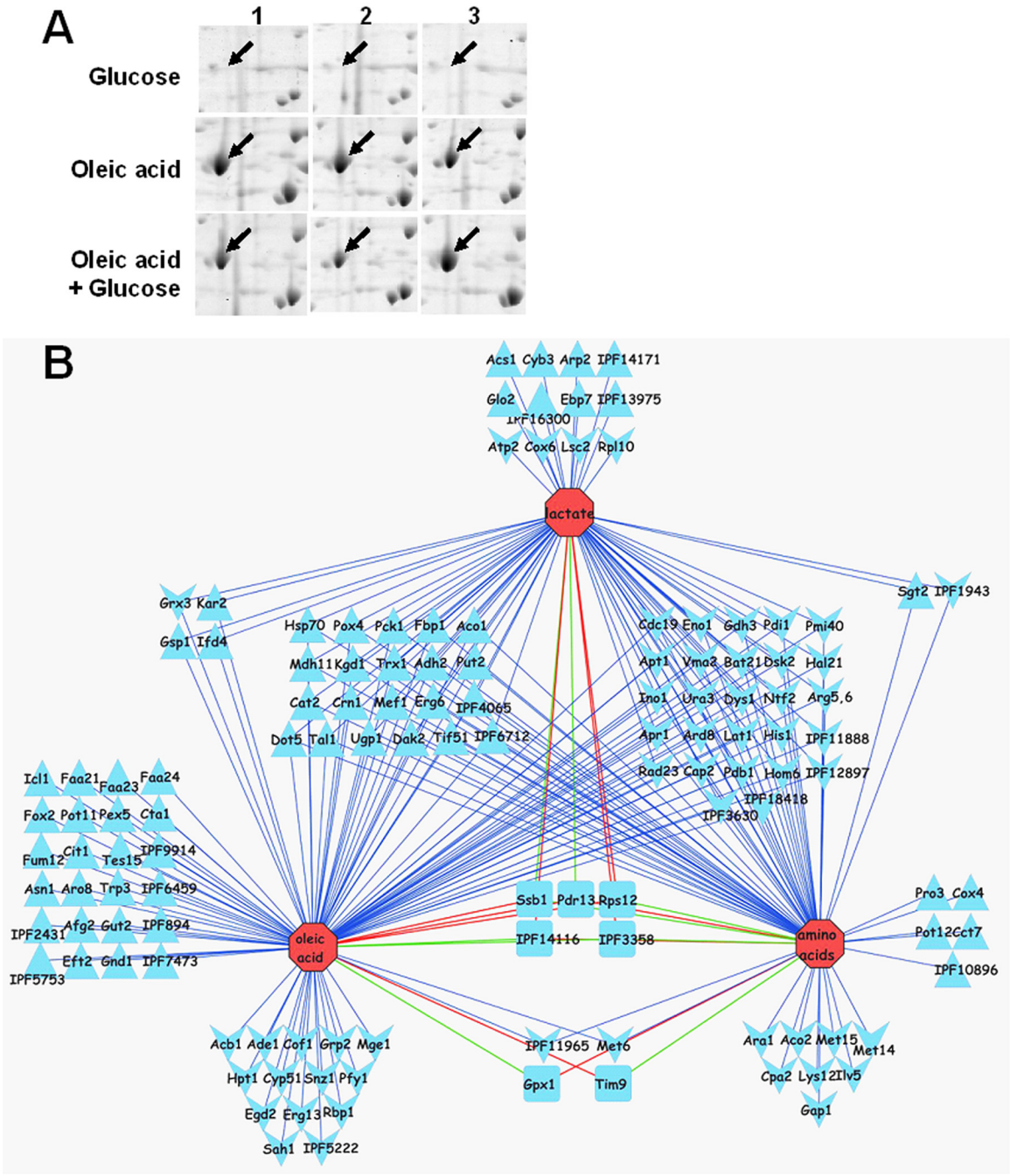

FIG 1 Impact of carbon source on the *C. albicans* proteome. (A) Replicate 2D gels showing that Pox4 is more abundant during growth on oleic acid than on glucose and that Pox4 is retained after 2 h of exposure to glucose. (B) Network of *C. albicans* proteins regulated in response to carbon source. Nodes are connected by edges to the one or more conditions under which it was identified: upregulated ≥2-fold relative to growth on glucose (upward arrowhead); downregulated ≥2-fold (downward arrowhead). Functions that were differentially regulated on different carbon sources (rounded rectangle) have color-coded connecting lines: green for upregulated and red for downregulated. Functions regulated under all three conditions lie in three blocks in the center of the network interactions.

upregulated (Fig. 1B and 2B; see Fig. S2 in the supplemental material). For example, gluconeogenic (Pck1 and Fbp1) and tricarboxylic acid cycle enzymes (Aco1, Kgd1, and Mdh11) displayed reduced levels, and the glycolysis-specific enzyme pyruvate kinase (Cdc19) was at elevated levels (see Fig. S2 and Table S2 in the supplemental material) during growth on glucose compared to lactate-, oleic acid-, and amino acid-grown cells. During growth on oleate, fatty acid β-oxidation (Faa21/23/24, Fox2, Pot11, Pox4, and Tes1), glyoxylate cycle (Icl1), and additional TCA cycle enzymes (Cit1 and Fum11) were present at elevated levels compared to the levels in glucose-grown cells (Fig. 2; Table S2). Enzymes on many amino acid biosynthetic pathways were downregulated during growth on amino acids (Arg5,6, Bat21, Cpa2, His1, Hom6, Ilv5, Lys12, and Met6/14/15), and this was also the case during

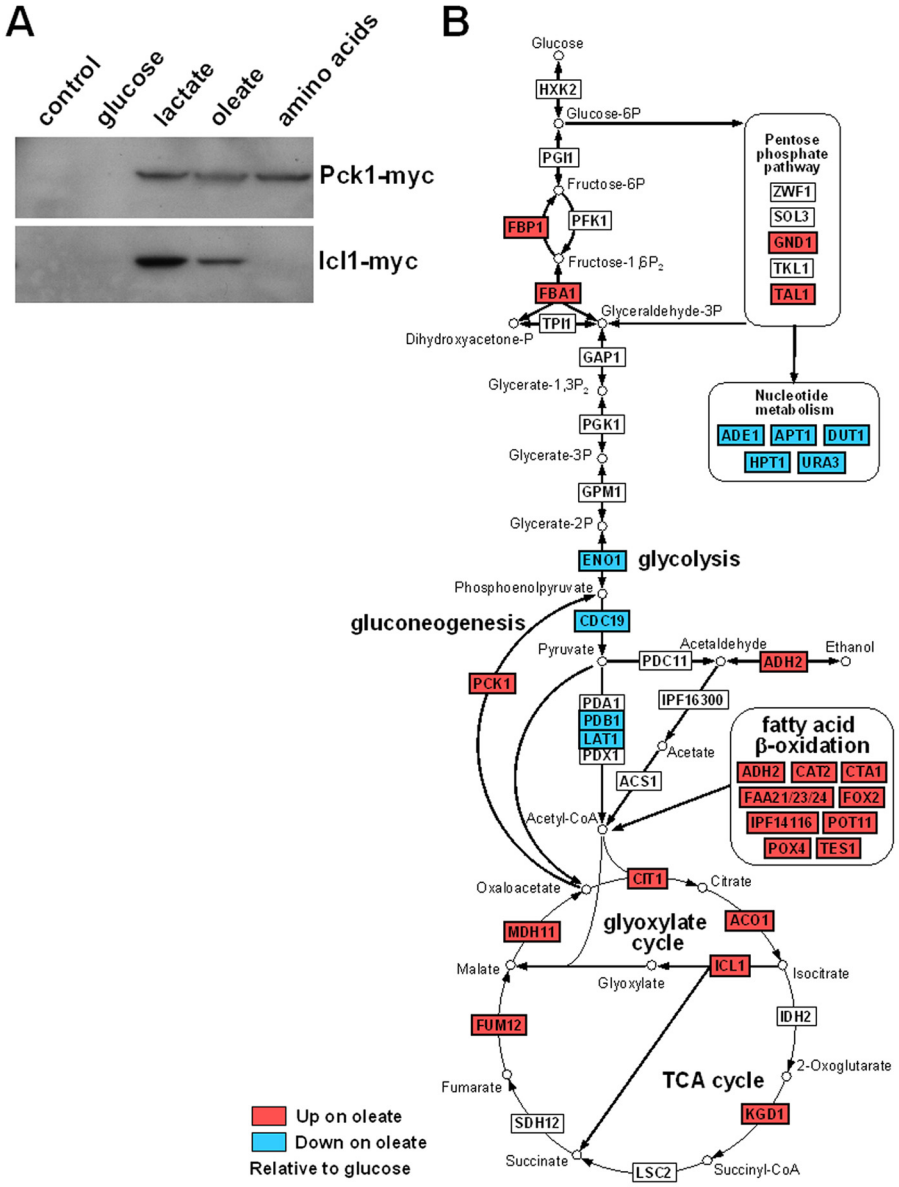

FIG 2 Effect of carbon source on central carbon metabolic enzymes in *C. albicans*. (A) Western blots demonstrating the effects of overnight growth on different carbon sources on the levels of Myc-tagged Icl1 and Pck1 in *C. albicans* cells (CA1395 and CA1431 [see Table S1 in the supplemental material]). Control lanes contain extracts from the untagged parental strain (RM1000) control grown on lactate. (B) Effects of growth on oleic acid versus glucose on the levels of enzymes involved in central carbon metabolism. All enzymes shown were identified on the 2D gels. The effects of growth on oleic acid versus glucose on the levels of enzymes are indicated as follows: white, no significant change in the levels of glucose- and oleic acid-grown cells; red, protein level significantly elevated in oleic acid-grown cells; cyan, protein level significantly elevated in glucose-grown cells. For abbreviations, see the *Candida* Genome Database (http://www.candidagenome.org).

growth on lactate (Arg5,6, Bat21, His1, and Met6) or oleic acid (Arg5,6, Bat21, His1, and Met6) (Fig. 1; Table S2). These data largely confirmed expectations based on our understanding of metabolism in other yeasts and the limited experimental data on *C. albicans* metabolic regulation (35, 49). The observed changes in Pck1 and Icl1 levels were validated by Western blot analysis of these proteins following Myc tagging in *C. albicans* (Fig. 2A). Note that Icl1 levels were below the limits of detection in the lactate proteome (Table S2).

The levels of other types of protein were modulated in response to carbon source. These proteins included proteins involved in growth and cell polarity (Arp2, Cap2, Pfy1, Cof1, Crn1, and Rbp1), nuclear transport (Ntf2), DNA repair (Rad23), and protein folding (Pdi1 and Cyp51) (see Table S2 in the supplemental material). Interestingly, proteins involved in drug resistance (Pdr13 and Erg13) were also affected by carbon source, which is consistent with the recent finding that carbon source affects the antifungal drug resistance of *C. albicans* (50). Also, a number of stress functions were affected by carbon source (Table S2). The levels of Hsp70 family members (Hsp70/Ssa4, Ssa1, and Kar2) were differentially regulated in response to carbon source. The Trx1 thioredoxin was also dramatically upregulated during

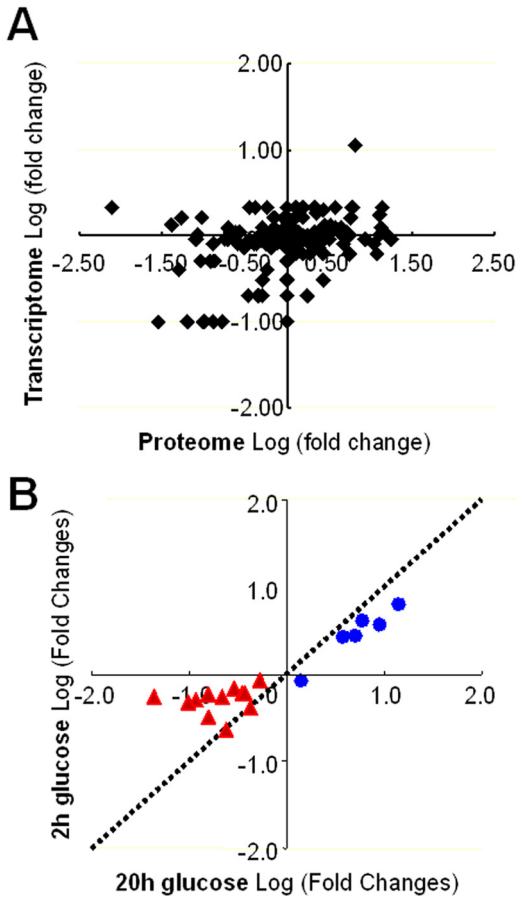

FIG 3 Comparisons of the *C. albicans* transcriptome and proteome. (A) The *C. albicans* transcriptome and proteome display limited correlation with respect to the observed log fold changes between cells grown on glucose or lactic acid. The transcriptomic data were taken from reference 47, and proteomic data were taken from Table S2 in the supplemental material. (B) Correlation between the short-term and long-term effects of glucose on central metabolic enzymes. Glycolytic enzymes are shown in blue. Gluconeogenic, glyoxylate cycle, and tricarboxylic acid (TCA) cycle enzymes are shown in red.

growth on lactate, oleic acid, or amino acids, while the glutaredoxin-like protein Grx3 was downregulated on lactate and oleic acid. The levels of catalase glutathione peroxidize (Gpx1) were also upregulated on lactate. These data were consistent with the observation that host carbon source affects stress resistance in *C. albicans* (50).

Transcript profiling data are available for the effects of glucose on lactate-grown *C. albicans* cells (47). We found the correlation between these transcript profiling data and our proteomic data for lactate- and glucose-grown cells to be modest at best (correlation coefficient = 0.25) (Fig. 3A). No doubt differential protein stabilities, alterations in posttranslational modifications, and the existence of multiple 2D gel features for some proteins contributed to this. Nevertheless, this was consistent with other comparisons of transcriptomic and proteomic data sets, which vary considerably in their degree of correlation (51–54).

Differential effects of glucose on the *C. albicans* proteome in the short term and longer term. Having tested the impact on the *C. albicans* proteome of growth on different carbon sources, we examined the effects of glucose addition to cells growing on alternative carbon sources. A similar experimental approach was taken except that *C. albicans* NGY152 cells were grown for 20 h to mid-exponential phase on lactate, oleate, or amino acids as the sole carbon source, and then 2% glucose was added 2 h before the cells were harvested for proteomic analyses. Once again, proteins that displayed statistically significant changes across three independent experiments (Fig. 1A) were identified by mass spectrometry (see Table S2 in the supplemental material; PRIDE accession numbers 3186 to 3192). Principal component analysis indicated that glucose addition exerted significant effects on the lactate, oleate, and amino acid proteomes and that these effects were distinct from long-term growth on glucose (Fig. 1B), although similar subsets of proteins were affected (Table S2).

We compared the short- and longer-term effects of glucose on the *C. albicans* proteome (Fig. 3B; see Fig. S1 in the supplemental material). Interestingly, the extent of correlation between the short- and long-term changes differed for different sets of functionally related proteins. Glycolytic enzymes showed a strong correlation, generally displaying glucose induction in both the short and longer terms (Fig. 3B). In contrast, gluconeogenic, glycoxylate cycle, TCA cycle, and fatty acid β-oxidation enzymes displayed a poor correlation. The levels of many of these enzymes were generally lower in glucose-grown cells, and their levels did not decline significantly after exposure to glucose for 2 h (Fig. S1).

Icl1 and Pck1 are not subject to catabolite inactivation in *C. albicans*. The apparent stability of gluconeogenic and glyoxylate cycle enzymes following glucose exposure in *C. albicans* contrasted with observations in *S. cerevisiae* where glucose triggers catabolite inactivation of these enzymes (23–25, 31). Therefore, we examined the impact of glucose on the stability of *C. albicans* Icl1 and Pck1 by Western blotting of Myc-tagged versions of these proteins (Fig. 4). *C. albicans* CA1395 (*ICL1-Myc*$_3$) and CA1431 (*PCK1-Myc*$_3$) (see Table S1 in the supplemental material) were grown to mid-exponential phase in medium containing lactate as the sole carbon source, and then 2% glucose was added. Protein extracts were prepared at various times thereafter and subjected to Western blotting, revealing that Icl1 and Pck1 were stable following glucose addition (Fig. 4B). Similar observations were made in oleic acid-grown cells exposed to glucose (see Fig. S3 in the supplemental material). These data were consistent with our observation that Icl1 and Pck1 are retained at high levels in *C. albicans* cells 2 h after glucose addition (Table S2).

We then measured the stability of the corresponding mRNAs under equivalent growth conditions by quantitative reverse transcription-PCR (qRT-PCR) relative to the internal *ACT1* mRNA control. The *ICL1* and *PCK1* mRNAs were rapidly degraded following glucose addition to lactate-grown cells (Fig. 4B), and similar data were obtained for oleic acid-grown cells (see Fig. S3 in the supplemental material). These observations were entirely consistent with the results of previous microarray experiments, suggesting that these transcripts are strongly repressed by glucose in *C. albicans* (46, 47). Therefore, *ICL1* and *PCK1* transcription is strongly regulated by glucose, but this regulation is not reflected in the proteome.

These experiments were replicated in *S. cerevisiae* to exclude the possibility that the lack of catabolite inactivation in *C. albicans* was an experimental artifact. *S. cerevisiae* DS1-W10 (*ICL1-Myc*$_9$) and DS1-W20 (*PCK1-HA*$_6$) (see Table S1 in the supplemental material) were grown on lactate and exposed to 2% glucose, and at various times thereafter, Icl1 and Pck1 levels were examined by

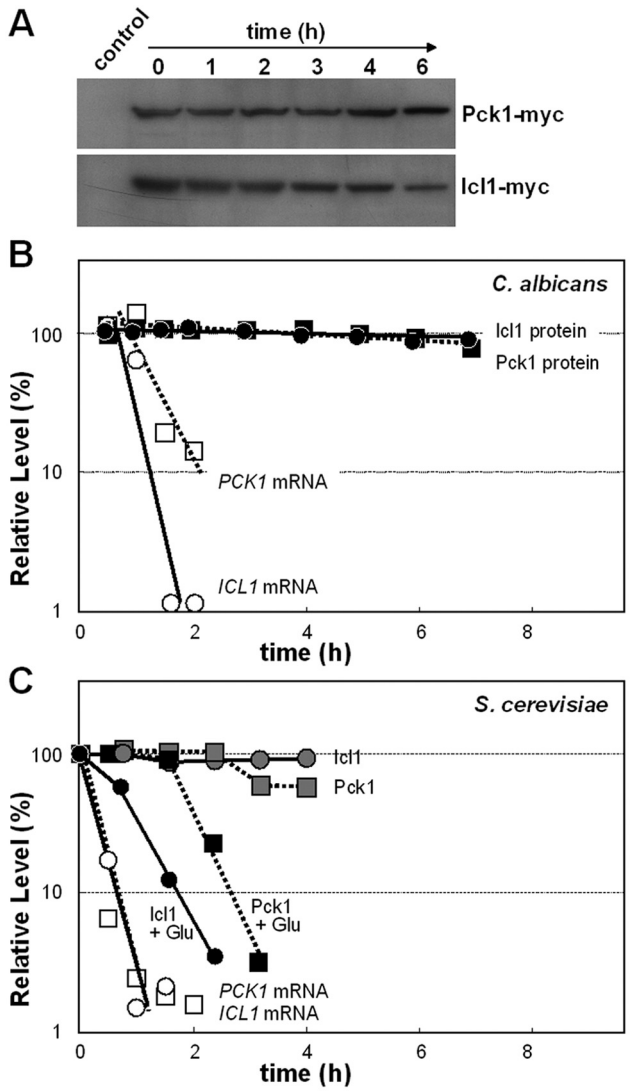

FIG 4 Icl1 and Pck1 protein stability and *ICL1* and *PCK1* mRNA turnover in *C. albicans* and *S. cerevisiae* following the addition of glucose. (A) CaIcl1-Myc and CaPck1-Myc protein levels were measured by Western blotting at various times after the addition of glucose to *C. albicans* cells grown on lactate. (B) CaIcl1-Myc and CaPck1-Myc were quantified by Western blotting relative to the Act1 internal control following glucose addition. Also *CaICL1* and *CaPCK1* mRNA levels were assayed in the same cultures by qRT-PCR and compared to the level in the *ACT1* mRNA internal control after glucose addition. The relative levels of these mRNAs and proteins were expressed as a percentage of their abundance at time zero, which was set at 100%. (C) ScIcl1-Myc and ScPck1-HA protein levels were measured by Western blotting, and *ScICL1* and *ScPCK1* mRNA levels were assayed by qRT-PCR in *S. cerevisiae* cells grown on lactate and exposed to glucose at time zero. The relative levels of these mRNAs and proteins were expressed as a percentage of their abundance at time zero (which was set at 100%): circles, Icl1; squares, Pck1; black symbols, Icl1 and Pck1 proteins in lactate-grown cells after glucose addition; gray symbols, Icl1 and Pck1 proteins in control lactate-grown cells with no glucose addition; open symbols, *ICL1* and *PCK1* mRNAs in lactate-grown cells after glucose addition. Similar data were obtained from two independent replicate experiments.

Western blotting (Fig. 4C). The Icl1 and Pck1 enzymes were stable in *S. cerevisiae* in the absence of glucose but were destabilized following glucose addition. Similar data were obtained for oleic acid-grown *S. cerevisiae* cells (see Fig. S3 in the supplemental material). These data recapitulate earlier observations (23, 24) and confirm that these gluconeogenic and glyoxylate cycle enzymes are subject to catabolite inactivation in *S. cerevisiae*. Furthermore, the *ICL1* and *PCK1* transcripts were rapidly degraded in *S. cerevisiae* following glucose addition (Fig. 4C), confirming earlier reports to this effect (5, 6, 20). Therefore, *C. albicans* differs significantly from *S. cerevisiae* in that Icl1 and Pck1 are not subject to catabolite inactivation in response to glucose in the pathogenic yeast.

***C. albicans* has retained the apparatus for catabolite inactivation.** In principle, the lack of glucose-accelerated degradation of Icl1 and Pck1 in *C. albicans* could have been due to the evolutionary loss of the catabolite inactivation apparatus in this pathogen. To test this, we asked whether *S. cerevisiae* Icl1 is subject to glucose-accelerated degradation in *C. albicans*.

C. albicans strains were constructed in which the *S. cerevisiae ICL1* (*ScICL1*) open reading frame (ORF) was expressed from the *C. albicans ICL1* (*CaICL1*) promoter at the native *ICL1* locus. The functionality of three-Myc (Myc_3)-tagged *S. cerevisiae* Icl1 (ScIcl1) in *C. albicans* was first confirmed in DSCO2 cells (*icl1/ScICL1*) (see Table S1 in the supplemental material), the *ScICL1-Myc_3* gene suppressing the growth defect of *C. albicans icl1* cells on lactate, oleic acid, pyruvate, and acetate as the sole carbon source (Fig. 5A). The stability of the Myc_3-tagged ScIcl1 was then examined in lactate-grown *C. albicans* DSCO1 cells (*ICL1/ScICL1-Myc_3*). ScIcl1 was stable in *C. albicans* in the absence of glucose but was rapidly degraded following glucose addition (Fig. 5B). These observations were reproducible, and analogous observations were made in oleic acid-grown *C. albicans* DSCO1 cells (see Fig. S4 in the supplemental material). We conclude that ScIcl1 is subject to glucose-accelerated degradation in *C. albicans*, and hence that during evolution *C. albicans* has retained the apparatus for catabolite inactivation.

In this case, has CaIcl1 lost the signal that triggers glucose-accelerated degradation? The stability of the CaIcl1-Myc_3 protein was assayed in the *S. cerevisiae* strain DS4-Y40 in which the Myc_3-tagged *CaICL1* open reading frame was expressed from the *ScICL1* promoter at the native *ICL1/YDR477w* locus (see Table S1 in the supplemental material). The CaIcl1-Myc_3 protein was stable in lactate-grown DS4-Y40 cells and was not destabilized by glucose addition relative to internal loading controls (Fig. 6). Once again, these observations were reproducible, and analogous observations were made for oleic acid-grown *S. cerevisiae* DS4-Y40 cells (see Fig. S4 in the supplemental material). Therefore, CaIcl1 appears to have lost the signal that triggers glucose-accelerated degradation.

Ubiquitination contributes to glucose-accelerated protein degradation in *C. albicans*. Ubiquitination contributes to glucose-mediated protein destabilization in *S. cerevisiae* (28, 32). Therefore, we tested whether ubiquitination contributes to glucose-accelerated degradation of ScIcl1 in *C. albicans*. The *ScICL1-Myc_3* cassette was integrated at the native *ICL1* locus in a *C. albicans ubi4* mutant that lacks polyubiquitin. Ubiquitination is significantly reduced in this *ubi4* mutant, residual ubiquitin being expressed only from the *UBI3* locus (55). The stability of the ScIcl1-Myc_3 protein in these *C. albicans* DSCO3 cells (*ubi4/ubi4 ICL1/ScICL1-Myc_3*) (see Table S1 in the supplemental material]) was compared to ScIcl1-Myc_3 stability in DSCO1 cells (*UBI4/UBI4 ICL1/ScICL1-Myc_3*) and the stability of the CaIcl1-Myc_3 protein in CA1395 cells (*UBI4/UBI4 ICL1/ICL1-Myc_3*). ScIcl1-Myc_3 and CaIcl1-Myc_3 were stable in these strains during growth

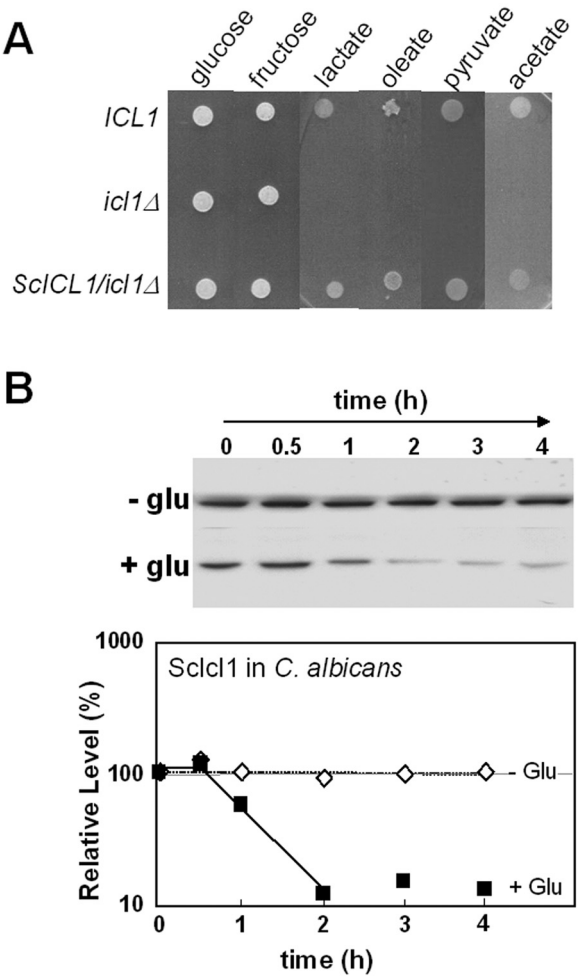

FIG 5 ScIcl1 is functional in *C. albicans* and rapidly degraded in response to glucose. (A) Expression of *ScICL1* in *C. albicans* suppresses the carbon source conditional phenotypes of an *icl1* mutant: *ICL1*, *C. albicans* CA510 (*ICL1/icl1*) (see Table S1 in the supplemental material); *icl1*, *C. albicans* CA517 (*icl1/icl1*); *ScICL1*, *C. albicans* DSCO1 (*ScICL1/icl1*). (B) Impact of glucose on the levels of the ScIcl1-Myc protein expressed in lactate-grown *C. albicans* DSCO1 cells relative to the abundance at time zero. (Top) Western blotting of ScIcl1-Myc levels. (Bottom) Quantification of ScIcl1-Myc levels expressed as a percentage of the abundance at time zero (100%): closed symbols, plus glucose; open symbols, control cells lacking glucose. Similar data were obtained from two independent replicate experiments.

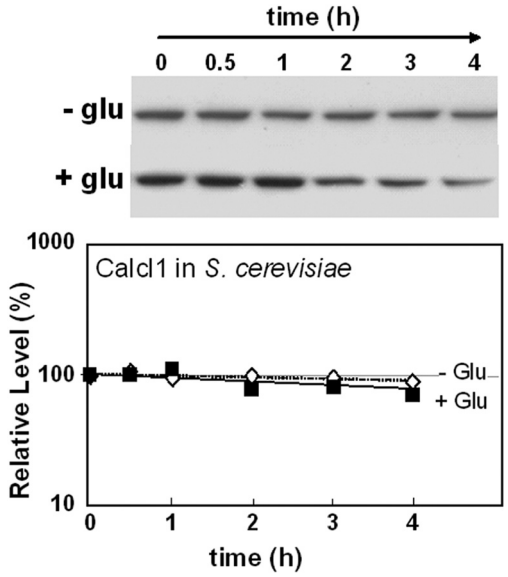

FIG 6 CaIcl1 is stable in *S. cerevisiae* following the addition of glucose. *CaICL1-Myc*$_3$ was expressed in *S. cerevisiae* DS4-Y40 cells (see Table S1 in the supplemental material) grown on lactate, and CaIcl1-Myc protein levels were assayed by Western blotting after glucose addition. CaIcl1-Myc levels are expressed as a percentage of the abundance at time zero (which was set at 100%): closed symbols, plus glucose; open symbols, control cells lacking glucose. Similar data were obtained from two independent replicate experiments.

on lactate in the absence of glucose (not shown). Once again, ScIcl1-Myc$_3$ was destabilized following glucose addition to wild-type DSCO1 cells (Fig. 7). However, ScIcl1-Myc$_3$ was partially stabilized in the polyubiquitin mutant, suggesting that glucose-accelerated degradation of ScIcl1 in *C. albicans* is at least partially dependent upon ubiquitination. This observation was reproducible in independent experiments, and furthermore, similar observations were made when the same strains were grown on oleic acid rather than lactate (see Fig. S5 in the supplemental material). The residual ScIcl1-Myc$_3$ destabilization observed in lactate- or oleic acid-grown *ubi4* cells could have been due either to the involvement of a second degradation pathway in this response (28) or to the residual ubiquitination that is observed in the *C. albicans* polyubiquitin mutant (55). We conclude that ubiquitination contributes to glucose-accelerated protein degradation in *C. albicans*.

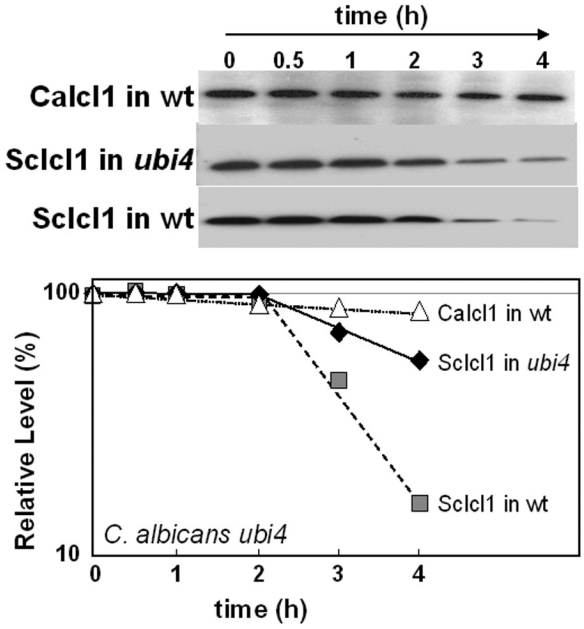

FIG 7 Inactivation of polyubiquitin inhibits glucose-accelerated ScIcl1 degradation in *C. albicans*. *ScICL1-Myc*$_3$ was expressed in *C. albicans* DSCO3 (*ubi4/ubi4*) (see Table S1 in the supplemental material) and DSCO1 (wild type [wt]) (*UBI4/UBI4*) cells grown on lactate, and then ScIcl1-Myc protein levels were assayed after the addition of glucose by Western blotting. For a control, CaIcI1-Myc levels were assayed in *C. albicans* DSCO3 (*ubi4/ubi4*) cells grown on lactate and following glucose addition. ScIcl1-Myc and CaIcl1-Myc levels are expressed as a percentage of their abundance at time zero (which was set at 100%). Similar data were obtained from two independent replicate experiments.

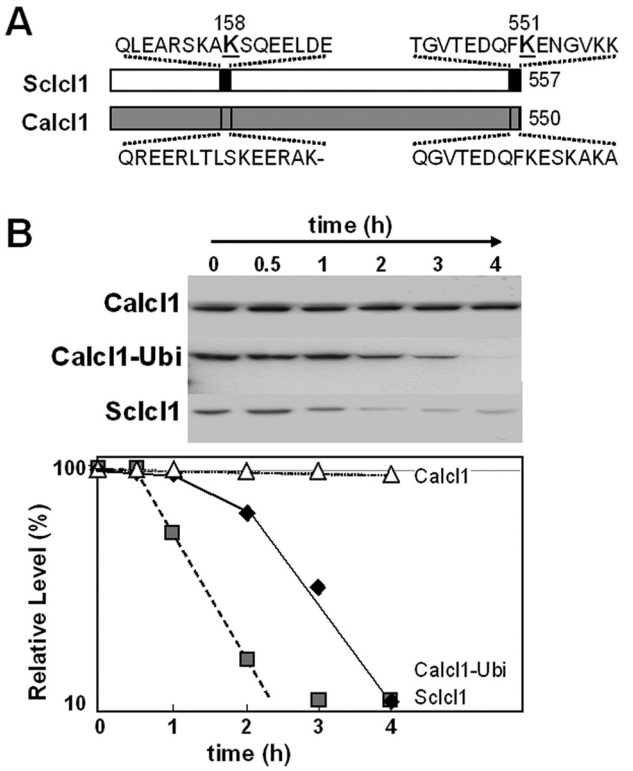

FIG 8 Addition of a consensus ubiquitin site stimulates glucose-accelerated degradation of CaICl1 in *C. albicans*. (A) Schematic representation illustrating the existence of high-confidence ubiquitination sites in ScIcl1 and the lack of such sites in CaIcl1 as predicted by UbPred (http://www.ubpred.org/index.html) (56). (B) The carboxy-terminal ubiquitination site from ScIcl1 was fused to CaIcl1 to create CaIcl1-Ubi-Myc in *C. albicans* DSCO4 (see Table S1 in the supplemental material). These cells were grown on lactate, and the levels of CaIcl1-Ubi-Myc were assayed by Western blotting after the addition of glucose. For controls, the stabilities of CaIcl1-Myc (CA1395) and ScIcl1-Myc (DSCO1) (gray squares) in *C. albicans* were compared under equivalent conditions. CaIcl1-Ubi-Myc, ScIcl1-Myc, and CaIcl1-Myc levels are expressed as a percentage of their abundance at time zero (which was set at 100%). Similar data were obtained from two independent replicate experiments.

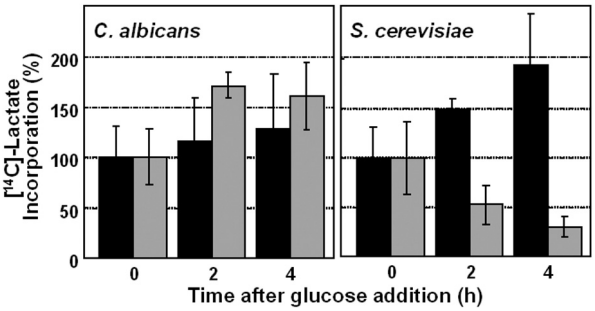

FIG 9 Glucose does not inhibit lactate assimilation by *C. albicans*. Exponential *C. albicans* RM1000 and *S. cerevisiae* W303-1B cells (see Table S1 in the supplemental material) grown on lactate were suspended in fresh medium containing [^{14}C]lactate and 2% glucose (gray bars) or with no glucose (black bars). The assimilation of radiolabeled lactate by cells was assayed at various times thereafter (Materials and Methods). Similar data were obtained from two independent replicate experiments.

***C. albicans* Icl1 lacks ubiquitination sites that trigger glucose-accelerated protein degradation.** Why does CaIcl1 escape glucose-accelerated ubiquitin-mediated protein degradation? We screened for consensus ubiquitination target sites in CaIcl1 and ScIcl1 using UbPred (predictor of protein ubiquitination sites) (http://www.ubpred.org/index.html) (56). The UbPred software, which was trained on 272 ubiquitination sites in *S. cerevisiae*, predicts ubiquitination sites based on numerous properties of the target amino acid sequence, including the net and total charge, aromatic content, charge/hydrophobicity ratio, sequence complexity, flexibility, amphipathic moment, and intrinsic disorder (56). The ScIcl1 and CaIcl1 proteins display strong amino acid sequence similarity (78% similarity and 67% identity). Yet while ScIcl1 contains two strong consensus ubiquitination sites at residues 158 and 551 according to UbPred, CaIcl1 carries no high-confidence ubiquitination targets (Fig. 8A). Therefore, we reasoned that the lack of such a ubiquitination site protected CaIcl1 from glucose-accelerated degradation.

To test this, we fused the carboxy-terminal ubiquitination site from ScIcl1 onto the carboxy terminus of CaIcl1 along with a Myc_3 epitope tag and then compared the stability of this CaIcl1-Ubi-Myc_3 protein with control CaIcl1-Myc_3 and ScIcl1-Myc_3 proteins in *C. albicans*. The stabilities of these proteins were first measured in mid-exponential *C. albicans* CA1395 (*ICL1/ICL1-Myc$_3$*), DSCO1 (*ICL1/ScICL1-Myc$_3$*), and DSCO4 (*ICL1/ICL1-Ubi-Myc$_3$*) cells grown on lactate. All of the proteins were stable under these conditions (not shown). Once again, ScIcl1-Myc_3 was destabilized following glucose addition, whereas CaIcl1-Myc_3 remained stable (Fig. 8B). Interestingly, the CaIcl1-Ubi-Myc_3 protein was reproducibly destabilized following glucose addition. Furthermore, analogous observations were made in *C. albicans* CA1395, DSCO1, and DSCO4 cells grown on oleic acid (see Fig. S6 in the supplemental material). Therefore, the addition of a ubiquitination site was sufficient to trigger glucose-accelerated degradation of the normally stable CaIcl1-Myc_3 protein in *C. albicans*. These observations reinforced the view that *C. albicans* has retained the apparatus for glucose-accelerated protein degradation and suggested that the lack of an appropriate ubiquitination site in CaIcl1 prevents this protein from entering this degradation pathway.

***C. albicans* continues to assimilate alternative carbon sources following glucose exposure.** Is this evolutionary rewiring of ubiquitination targets between *C. albicans* and *S. cerevisiae* reflected in the metabolic activities of these yeasts? To test this, we compared [^{14}C]lactate assimilation by mid-exponential *C. albicans* RM1000 and *S. cerevisiae* W303-1B cells that were grown on lactate in the presence and absence of glucose (Fig. 9). As expected, the presence of glucose inhibited the assimilation of [^{14}C]lactate by *S. cerevisiae*. However, glucose did not inhibit [^{14}C]lactate by *C. albicans* over the 4-h period examined, which was consistent with the retention by this pathogen of glyoxylate cycle and gluconeogenic enzymes after glucose addition. These reproducible observations were reinforced by analogous data on oleic acid assimilation by oleic acid-grown *C. albicans* and *S. cerevisiae* cells. Glucose inhibited [^{3}H]oleic acid assimilation in *S. cerevisiae* W303-1B cells, but not in *C. albicans* RM1000 cells (see Fig. S7 in the supplemental material). These data indicate that, unlike *S. cerevisiae*, *C. albicans* continues to assimilate alternative carbon sources after exposure to glucose.

DISCUSSION

The prevailing view is that *C. albicans* fits the *S. cerevisiae* paradigm with regard to the impact of glucose upon central carbon metabolism. This influences current thinking about nutrient adaptation during infection and host-fungus interactions (46, 47, 57). However, this view does not resonate well with the evolution of these yeasts in contrasting niches that differ significantly with regard to carbon source availability (40) and with an early report that *C. albicans* is a Crabtree-negative yeast (48). We now show that, despite the similar effects that glucose exerts on the *C. albicans* and *S. cerevisiae* transcriptomes (46, 47), these yeasts display fundamental differences in the effects of glucose on central metabolic functions and carbon assimilation. The levels of many gluconeogenic, glyoxylate cycle, and fatty acid β-oxidation enzymes do decline in *C. albicans* after protracted growth on glucose, and the changes in the proteomic network (Fig. 1) reflect those observed previously during a comprehensive comparison of exponential- and stationary-phase *C. albicans* cells (58). However, these enzymes are stable during short-term exposure to glucose (Fig. 2 and 4; see Table S2 in the supplemental material), and this allows *C. albicans* cells to continue to assimilate alternative carbon sources even in the presence of glucose, unlike *S. cerevisiae* (Fig. 9).

Our analyses of Icl1 and Pck1 turnover have suggested that enzymes involved in the assimilation of alternative carbon sources are retained in *C. albicans* following glucose addition because these enzymes remain stable while their transcripts are degraded (Fig. 4). We show that this contrasts with *S. cerevisiae* cells that degrade these enzymes following glucose addition and their transcripts (Fig. 4). It is conceivable that carboxy-terminal tagging of CaIcl1 and ScIcl1 affected their localization and stability. Nevertheless, our data were consistent with the study of López-Boado et al. (24) who reported that Icl1 is subject to catabolite inactivation in *S. cerevisiae*. We then showed that, although CaIcl1 and CaPck1 are not subjected to glucose-accelerated protein degradation in *C. albicans*, this pathogen has retained the molecular apparatus to execute this function, as ScIcl1 is degraded following glucose addition when expressed as a functional enzyme in *C. albicans* (Fig. 5). Rather, CaIcl1 lacks the signal that triggers glucose-accelerated protein degradation in *S. cerevisiae* (Fig. 6).

Ubiquitin-dependent mechanisms contribute to the catabolite inactivation of Fbp1 in *S. cerevisiae* (28), and protein ubiquitination is known to be important for nutrient adaptation as well as growth, morphogenesis, and stress responses in *C. albicans* (55, 59–64). Therefore, we reasoned that ubiquitination might also contribute to glucose-accelerated protein degradation in *C. albicans* and that CaIcl1 might lack critical ubiquitination sites required to target this protein for catabolite inactivation. Three observations support this hypothesis. First, the inactivation of polyubiquitin (Ubi4) lowered the rate of ScIcl1 degradation in *C. albicans* (Fig. 7). ScIcl1 degradation was not completely blocked because the *UBI3* gene would provide residual ubiquitin in *C. albicans ubi4* cells (55, 65). Second, *in silico* analyses of the ScIcl1 and CaIcl1 sequences revealed that while ScIcl1 contains two high-confidence ubiquitination sites, CaIcl1 contains none (Fig. 8A) despite these proteins displaying a high degree of overall sequence identity (67%). Third, the addition of a carboxy-terminal ubiquitination site to the CaIcl1 protein was sufficient to program this protein for glucose-accelerated protein degradation in *C. albicans* (Fig. 8). Therefore, during the evolution of *C. albicans*, this pathogen has retained the molecular apparatus that mediates glucose-accelerated protein degradation, and CaIcl1 has evolved to escape this process.

Our proteomic analyses indicate that other *C. albicans* enzymes involved in the assimilation of alternative carbon sources lack ubiquitination sites are retained following glucose exposure (Fig. 3B; see Table S1 in the supplemental material). Furthermore, our *in silico* comparisons have suggested that enzymes specific for gluconeogenesis and the glyoxylate cycle lack the requisite ubiquitination sites required for glucose-accelerated protein degradation. *S. cerevisiae* malate synthase (ScMls1) contains three low-confidence ubiquitination sites according to UbPred (http://www.ubpred.org/index.html) (56), whereas CaMls1 contains no putative ubiquitination sites. UbPred also predicts that both ScFbp1 and ScPck1 contain high-confidence ubiquitination sites, whereas CaFbp1 and CaPck1 do not. This was consistent with our observation that, following glucose addition, ScPck1 is degraded in *S. cerevisiae*, but CaPck1 is not degraded in *C. albicans* (Fig. 4). Meanwhile, our previous work has indicated that a number of glycolytic enzymes are ubiquitinated in *C. albicans* (55). Therefore, significant evolutionary rewiring of ubiquitination targets appears to have occurred in this pathogen, allowing it to assimilate alternative carbon sources in the presence of glucose, unlike *S. cerevisiae* (Fig. 9).

These observations have several important implications for our understanding of *C. albicans* as a pathogen. First, our data indicate that under some conditions there is significant dislocation between the transcriptome and proteome. Microarray studies have contributed significantly to our understanding of *C. albicans* pathobiology (43, 44, 46, 66–68), and it is frequently presumed that changes in the transcriptome are reflected in corresponding changes in the *C. albicans* proteome and physiology. In some cases, there is a good correlation between the transcriptome and proteome, for example with regard to the induction of glycolytic enzymes in response to glucose (Fig. 3) and during amino acid starvation (54). However, this is not always the case (69), and this study demonstrates clearly that caution is required in making presumptions about the proteome based on the transcriptome. Indeed, this explains the conundrum as to why *C. albicans* is a Crabtree-negative yeast (48) even though its transcriptome is exquisitely sensitive to glucose (47). Thankfully, many studies provide experimental confirmation of working hypotheses on the basis of their microarray observations.

The second important implication relates to fungal nutrient assimilation during colonization and disease progression. *C. albicans* occupies dynamic host niches that contain complex mixtures of carbon sources that change over time through a combination of host and fungal metabolic activities. Many niches contain minimal sugar concentrations (e.g., the urogenital tract), while in others, *C. albicans* is transiently exposed to sugars (e.g., the oral cavity and gastrointestinal tract). This opportunistic pathogen probably evolved in niches such as these. Also, the evidence suggests that a proportion of *C. albicans* cells that infect internal organs actively assimilate alternative carbon sources rather than sugars (40, 70). Furthermore, lactate assimilation is essential for the proliferation of *C. glabrata* in the intestine (38). Our data now suggest that transient exposure to sugar does not prejudice the assimilation of alternative carbon sources and, as a result, the growth of the fungus in these niches. This explains why both gluconeogenic and glycolytic functions can be expressed in *C. albicans* cells infecting

the kidney (40) and why mutations that block gluconeogenesis or the glyoxylate cycle partially attenuate the virulence of *C. albicans* (39–42). Clearly, *C. albicans* does not conform to the *S. cerevisiae* paradigm of glucose regulation, and this is important for the pathogenicity of this yeast.

MATERIALS AND METHODS

Strains and growth conditions. *C. albicans* and *S. cerevisiae* strains (see Table S1 in the supplemental material) were grown at 30°C in minimal medium (0.67% yeast nitrogen base) containing glucose (2%) (SD), lactic acid (2%), oleic acid (0.2%), or mixed amino acids (2%) as the sole carbon source (71).

Strain construction. *C. albicans* strains expressing Icl1-Myc_3 (CA1395) or Pck1-Myc_3 (CA1431) were made by PCR amplification of a *Myc_3-URA3* cassette and transforming these products into *C. albicans* RM1000 (see Table S1 in the supplemental material). Insertion at the correct locus was confirmed by diagnostic PCR, and expression of Icl1-Myc_3 and Pck1-Myc_3 was confirmed by Western blotting. Analogous controls were performed for all the following strain constructions.

To replace a *CaICL1* allele in *C. albicans* with a Myc_3-tagged *ScICL1* open reading frame (ORF) from *S. cerevisiae*, the *ScICL1* locus was first Myc_3 tagged by PCR amplifying the *Myc_3-URA3* cassette with primers DS_3F (F stands for forward) and DS_3R (R stands for reverse) (see Table S3 in the supplemental material) and transforming this cassette into *S. cerevisiae* BY4743 to create strain DS3-Y30 (Table S1). The new *ScICL1-Myc_3-URA3* locus was then PCR amplified using primers DS_5F and DS_5R, and this *CaICL1p-ScICL1-MYC_3-URA3* cassette was then transformed into *C. albicans* RM1000 to create strain DSCO1 (*CaICL1/CaICL1p-ScICL1-MYC_3-URA3*) (Table S1) and also transformed into *C. albicans* CA510 to create strain DSCO1 (*Caicl1/CaICL1p-ScICL1-MYC_3-URA3*) (Table S1).

To introduce the *CaICl1-ScICL1-Myc_3-URA3* allele into the *C. albicans ubi4/ubi4* background (55), the *CaICl1-ScICL1-Myc_3-URA3* cassette was PCR amplified using the DS_5F and DS_5R primers (see Table S3 in the supplemental material) and transformed into *C. albicans* DSCO to create strain DSCO3 (*ubi4/ubi4 CaICL1/CaICl1-ScICL1-Myc_3-URA3*) (Table S1).

C. albicans DSCO4 expresses CaIcl1 with the carboxy-terminal ubiquitination site from ScIcl1 at its carboxy terminus (*CaICL1/CaICl1-Ubi-Myc_3-URA3*) (see Table S1 in the supplemental material). This was achieved by PCR amplifying the 3′ end of the *ScICL1* ORF along with the conjoined *MYC3-URA3* sequences from *S. cerevisiae* DSCO3 cells using the DS_6F and DS_6Rprimers (Table S3) and transforming this *CaICl1-Ubi-Myc_3-URA3* cassette into *C. albicans* RM1000.

The *ScICL1* and *ScPCK1* loci were epitope tagged in *S. cerevisiae*. *ScICL1* was tagged with Myc_9 at its 3′ end by PCR amplification of the *MYC_9-NAT* cassette in pYM21 (72) with primers DS_1F and DS_1R (see Table S3 in the supplemental material) and transformation of *S. cerevisiae* W303-1B to generate strain DS1-W10 (*ScICL1-MYC_9-NAT*) (Table S1). *ScPCK1* was tagged with hemagglutinin (a six-hemagglutinin tag [HA_6]) by PCR amplification of the *HA_6-KlTRP1* (*KlTRP1* stands for *Kluyveromyces lactis TRP1*) cassette in pYM3 (73) with primers DS_2F and DS_2R (Table S3) and transformation of *S. cerevisiae* W303-1B to create strain DS1-W20 (*ScPCK1-HA_6-KlTRP1*) (Table S1).

The *ScICl1* ORF in *S. cerevisiae* BY4743 was replaced with *CaICL1-Myc_3* to create the *S. cerevisiae* strain DS4-Y40 (*ScICl1-CaICL1-Myc_3-URA3*) (see Table S1 in the supplemental material). The *CaICL1-Myc_3-URA3* ORF was PCR amplified from *C. albicans* CA1395 (Table S1) using the DS_4F and DS_4R primers (Table S3).

Proteomics. Replicate cultures of *C. albicans* NGY152 (CAI4 containing CIp10 [74]) were grown in minimal medium containing glucose (2%), lactic acid (2%), oleic acid (0.2%), or mixed amino acids (2%) as the sole carbon source. Samples from the cultures were taken, then subcultured in the same medium, grown for a further 20 h, and harvested in exponential phase (optical density at 600 nm [OD_{600}] of 0.8). Glucose (2%) was added to some cultures, and the cells were harvested after 2 h. Protein extracts were prepared, subjected to 2D gel electrophoresis, and stained with Coomassie blue as described previously (54). Independent triplicate experiments were done for each growth condition. Gel features were compared using *Phoretix* 2D Expression (Nonlinear Dynamics, Newcastle upon Tyne, United Kingdom) and GeneSpring (Silicon Genetics, San Carlos, CA). Principal component analysis scores were plotted in 3D (SIMCA-P version 11.0: Umetrics AB, Sweden). Proteins displaying statistically significant differences in mean spot volume ($P \leq 0.05$) were identified by MALDI-ToF mass spectrometry of tryptic peptides (54) using MS-Fit and MASCOT (Matrix Science, Boston, MA). Protein annotations were from the *Candida* Genome Database (http://www.candidagenome.org/). The proteomic data set is available in the supplemental material (see Table S2 in the supplemental material) and at the PRIDE proteomic data repository (http://www.ebi.ac.uk/pride/) (accession numbers 3186 to 3192). The carbon source network was constructed using Cytoscape version (http://www.cytoscape.org/) (75).

Western blotting. Protein extracts were subjected to Western blotting as described previously (76). Membranes were probed with a mouse anti-Myc antibody (diluted 1:10,000) (Sigma). The secondary antibody was peroxidase-conjugated rabbit anti-mouse IgG. Signals were detected with an enhanced chemiluminescence (ECL) Western blotting kit (Amersham, United Kingdom) and quantified using a Fuji FLA-3000 imager.

RNA analyses. RNA was prepared (77, 78), yields were quantified using an RNA 6000 Nano assay, and RNA integrity was assessed using an Agilent 2100 bioanalyzer (79). *ICL1* and *PCK1* transcript levels were quantified to the internal *ACT1* mRNA by qRT-PCR using primers (see Table S3 in the supplemental material). RNA samples (2 μg) were incubated in 20-μl reactions with DNase I (1.5 μl), RNase OUT (1.5 μl), and DNase I buffer (2 μl) (Invitrogen, United Kingdom) at room temperature for 15 min. cDNA was then made with SuperScript II reverse transcriptase (Invitrogen, United Kingdom) following the manufacturer's protocols. Real-time RT-PCR SYBR green (Roche, United Kingdom) was performed using the manufacturer's instructions with a LightCycler 480 real-time PCR system (Roche).

Lactate and oleic acid assimilation. Lactate and oleic acid assimilation was assayed by measuring the incorporation by *C. albicans* and *S. cerevisiae* of [^{14}C]lactate and [^{3}H]oleic acid into trichloroacetic acid-precipitable material. Yeast cells were grown on YPLactate (2% Bacto peptone and 1% yeast extract containing 2% lactate) or YPOleic acid (2% Bacto peptone and 1% yeast extract containing 0.2% oleic acid) at 30°C to an OD_{600} of 1, harvested, and resuspended in 1 ml fresh prewarmed YP-Lactate or YPOleic acid. Glucose (2%) was added to half of the cells, and no glucose was added to control cells. Then, 1.85 MBq of [^{14}C]lactic acid or 37 MBq of [^{3}H]oleic acid was added at time zero, and samples were taken at various times thereafter. The samples were precipitated in 5% trichloroacetic acid at 0°C, washed at 0°C in a series of solutions [(i) fresh 5% trichloroacetic acid containing 0.1% SDS, (ii) 50% ethanol, and (iii) 100% ethanol], dried, and subjected to scintillation counting (Packard BioScience). The results are means and standard deviations from triplicate assays. Similar results were obtained in triplicate independent experiments.

SUPPLEMENTAL MATERIAL

Supplemental material for this article may be found at http://mbio.asm.org/lookup/suppl/doi:10.1128/mBio.00495-12/-/DCSupplemental.

Figure S1, PDF file, 0.1 MB.
Figure S2, PDF file, 0.1 MB.
Figure S3, PDF file, 0.1 MB.
Figure S4, PDF file, 0.1 MB.
Figure S5, PDF file, 0.1 MB.
Figure S6, PDF file, 0.1 MB.
Figure S7, PDF file, 0.1 MB.
Table S1, PDF file, 0.1 MB.
Table S2, PDF file, 0.1 MB.
Table S3, PDF file, 0.1 MB.

ACKNOWLEDGMENTS

We thank Esperanza Lopez-Franco for help with the construction of *C. albicans* Pck1-Myc and Icl1-Myc strains. We thank Phil Cash, Mike Lorenz, and Ben Distel for stimulating discussions and helpful advice. D.S. was supported by a scholarship from Universiti Sains, Malaysia. M.D.L. was the recipient of a Carnegie/Caledonian scholarship from the Carnegie Trust, and a Sir Henry Wellcome postdoctoral fellowship from the Wellcome Trust (096072). This work was also supported by the United Kingdom Biotechnology and Biological Research Council (BBS/B/06679 and BB/F00513X/1), the Wellcome Trust (080088 and 097377), and the European Commission (PITN-GA-2008-214004 and ERC-2009-AdG-249793).

REFERENCES

1. **Jacob F, Monod J.** 1961. Genetic regulatory mechanisms in the synthesis of proteins. J. Mol. Biol. **3**:318–356.
2. **Beckwith JR.** 1967. Regulation of the lac operon. Recent studies on the regulation of lactose metabolism in *Escherichia coli* support the operon model. Science **156**:597–604.
3. **Crabtree HG.** 1928. The carbohydrate metabolism of certain pathological overgrowths. Biochem. J. **22**:1289–1298.
4. **Barford JP, Hall RJ.** 1978. An examination of the Crabtree effect in *Saccharomyces cerevisiae*: the role of respiratory adaptation. J. Gen. Microbiol. **114**:267–275.
5. **Yin Z, Smith RJ, Brown AJ.** 1996. Multiple signalling pathways trigger the exquisite sensitivity of yeast gluconeogenic mRNAs to glucose. Mol. Microbiol. **20**:751–764.
6. **Yin Z, et al.** 2003. Glucose triggers different global responses in yeast, depending on the strength of the signal, and transiently stabilizes ribosomal protein mRNAs. Mol. Microbiol. **48**:713–724.
7. **Gancedo JM.** 1998. Yeast carbon catabolite repression. Microbiol. Mol. Biol. Rev. **62**:334–361.
8. **Carlson M.** 1999. Glucose repression in yeast. Curr. Opin. Microbiol. **2**:202–207.
9. **Johnston M.** 1999. Feasting, fasting and fermenting. Glucose sensing in yeast and other cells. Trends Genet. **15**:29–33.
10. **Thevelein JM, de Winde JH.** 1999. Novel sensing mechanisms and targets for the cAMP-protein kinase A pathway in the yeast *Saccharomyces cerevisiae*. Mol. Microbiol. **33**:904–918.
11. **Rolland F, Winderickx J, Thevelein JM.** 2001. Glucose-sensing mechanisms in eukaryotic cells. Trends Biochem. Sci. **26**:310–317.
12. **Gancedo JM.** 2008. The early steps of glucose signalling in yeast. FEMS Microbiol. Rev. **32**:673–704.
13. **Gounalaki N, Thireos G.** 1994. Yap1p, a yeast transcriptional activator that mediates multidrug resistance, regulates the metabolic stress response. EMBO J. **13**:4036–4041.
14. **Görner W, et al.** 1998. Nuclear localization of the C2H2 zinc finger protein Msn2p is regulated by stress and protein kinase A activity. Genes Dev. **12**:586–597.
15. **Stanhill A, Schick N, Engelberg D.** 1999. The yeast ras/cyclic AMP pathway induces invasive growth by suppressing the cellular stress response. Mol. Cell. Biol. **19**:7529–7538.
16. **Garreau H, et al.** 2000. Hyperphosphorylation of Msn2p and Msn4p in response to heat shock and the diauxic shift is inhibited by cAMP in *Saccharomyces cerevisiae*. Microbiology **146**(Part 9):2113–2120.
17. **Ozcan S, Johnston M.** 1999. Function and regulation of yeast hexose transporters. Microbiol. Mol. Biol. Rev. **63**:554–569.
18. **Kaniak A, Xue Z, Macool D, Kim JH, Johnston M.** 2004. Regulatory network connecting two glucose signal transduction pathways in *Saccharomyces cerevisiae*. Eukaryot. Cell **3**:221–231.
19. **Usaite R, et al.** 2009. Reconstruction of the yeast Snf1 kinase regulatory network reveals its role as a global energy regulator. Mol. Syst. Biol. **5**:319.
20. **Mercado JJ, Smith R, Sagliocco FA, Brown AJ, Gancedo JM.** 1994. The levels of yeast gluconeogenic mRNAs respond to environmental factors. Eur. J. Biochem. **224**:473–481.
21. **Scheffler IE, de la Cruz BJ, Prieto S.** 1998. Control of mRNA turnover as a mechanism of glucose repression in *Saccharomyces cerevisiae*. Int. J. Biochem. Cell Biol. **30**:1175–1193.
22. **Ashe MP, De Long SK, Sachs AB.** 2000. Glucose depletion rapidly inhibits translation initiation in yeast. Mol. Biol. Cell **11**:833–848.
23. **Entian KD, Dröll L, Mecke D.** 1983. Studies on rapid reversible and non-reversible inactivation of fructose-1,6-bisphosphatase and malate dehydrogenase in wild-type and glycolytic block mutants of *Saccharomyces cerevisiae*. Arch. Microbiol. **134**:187–192.
24. **López-Boado YS, Herrero P, Gascón S, Moreno F.** 1987. Catabolite inactivation of isocitrate lyase from *Saccharomyces cerevisiae*. Arch. Microbiol. **147**:231–234.
25. **Hämmerle M, et al.** 1998. Proteins of newly isolated mutants and the amino-terminal proline are essential for ubiquitin-proteasome-catalyzed catabolite degradation of fructose-1,6-bisphosphatase of *Saccharomyces cerevisiae*. J. Biol. Chem. **273**:25000–25005.
26. **Jiang H, Tatchell K, Liu S, Michels CA.** 2000. Protein phosphatase type-1 regulatory subunits Reg1p and Reg2p act as signal transducers in the glucose-induced inactivation of maltose permease in *Saccharomyces cerevisiae*. Mol. Gen. Genet. **263**:411–422.
27. **Horak J, Regelmann J, Wolf DH.** 2002. Two distinct proteolytic systems responsible for glucose-induced degradation of fructose-1,6-bisphosphatase and the Gal2p transporter in the yeast *Saccharomyces cerevisiae* share the same protein components of the glucose signaling pathway. J. Biol. Chem. **277**:8248–8254.
28. **Regelmann J, et al.** 2003. Catabolite degradation of fructose-1,6-bisphosphatase in the yeast *Saccharomyces cerevisiae*: a genome-wide screen identifies eight novel GID genes and indicates the existence of two degradation pathways. Mol. Biol. Cell **14**:1652–1663.
29. **Mercado JJ, Vincent O, Gancedo JM.** 1991. Regions in the promoter of the yeast *FBP1* gene implicated in catabolite repression may bind the product of the regulatory gene *MIG1*. FEBS Lett. **291**:97–100.
30. **Mercado JJ, Gancedo JM.** 1992. Regulatory regions in the yeast *FBP1* and *PCK1* genes. FEBS Lett. **311**:110–114.
31. **Gancedo JM, Gancedo C.** 1997. Gluconeogenesis and catabolite inactivation, p 359–377. *In* Zimmermann FK, Entian KD (ed), Yeast sugar metabolism. Technomic Publishing, Basel, Switzerland.
32. **Schüle T, Rose M, Entian KD, Thumm M, Wolf DH.** 2000. Ubc8p functions in catabolite degradation of fructose-1,6-bisphosphatase in yeast. EMBO J. **19**:2161–2167.
33. **Sabina J, Brown V.** 2009. Glucose sensing network in *Candida albicans*: a sweet spot for fungal morphogenesis. Eukaryot. Cell **8**:1314–1320.
34. **Merico A, Sulo P, Piskur J, Compagno C.** 2007. Fermentative lifestyle in yeasts belonging to the *Saccharomyces* complex. FEBS J. **274**:976–989.
35. **Odds FC.** 1988. *Candida* and candidosis. Bailliere Tindall, London, United Kingdom.
36. Calderone RA (ed). 2002. *Candida* and candidiasis. ASM Press, Washington, DC.
37. **Buchalter SE, Crain MR, Kreisberg R.** 1989. Regulation of lactate metabolism in vivo. Diabetes Metab. Rev. **5**:379–391.
38. **Ueno K, et al.** 2011. Intestinal resident yeast *Candida glabrata* requires Cyb2p-mediated lactate assimilation to adapt in mouse intestine. PLoS One **6**:e24759.
39. **Lorenz MC, Fink GR.** 2001. The glyoxylate cycle is required for fungal virulence. Nature **412**:83–86.
40. **Barelle CJ, et al.** 2006. Niche-specific regulation of central metabolic pathways in a fungal pathogen. Cell. Microbiol. **8**:961–971.
41. **Piekarska K, et al.** 2006. Peroxisomal fatty acid beta-oxidation is not essential for virulence of *Candida albicans*. Eukaryot. Cell **5**:1847–1856.
42. **Ramírez MA, Lorenz MC.** 2007. Mutations in alternative carbon utilization pathways in *Candida albicans* attenuate virulence and confer pleiotropic phenotypes. Eukaryot. Cell **6**:280–290.
43. **Ihmels J, et al.** 2005. Rewiring of the yeast transcriptional network through the evolution of motif usage. Science **309**:938–940.
44. **Martchenko M, Levitin A, Hogues H, Nantel A, Whiteway M.** 2007. Transcriptional rewiring of fungal galactose-metabolism circuitry. Curr. Biol. **17**:1007–1013.
45. **Lavoie H, Hogues H, Whiteway M.** 2009. Rearrangements of the transcriptional regulatory networks of metabolic pathways in fungi. Curr. Opin. Microbiol. **12**:655–663.
46. **Lorenz MC, Bender JA, Fink GR.** 2004. Transcriptional response of *Candida albicans* upon internalization by macrophages. Eukaryot. Cell **3**:1076–1087.
47. **Rodaki A, et al.** 2009. Glucose promotes stress resistance in the fungal pathogen *Candida albicans*. Mol. Biol. Cell **20**:4845–4855.
48. **Niimi M, Kamiyama A, Tokunaga M.** 1988. Respiration of medically important *Candida* species and *Saccharomyces cerevisiae* in relation to glucose effect. J. Med. Vet. Mycol. **26**:195–198.
49. **Brown AJ.** 2005. Integration of metabolism with virulence in *Candida*

albicans, p 185–203. *In* Brown AJ (ed.), Fungal genomics. Mycota XIII. Springer-Verlag, Heidelberg, Germany.
50. **Ene IV, et al.** 2012. Host carbon sources modulate cell wall architecture, drug resistance and virulence in a fungal pathogen. Cell. Microbiol. **14**: 1319–1335.
51. **Futcher B, Latter GI, Monardo P, McLaughlin CS, Garrels JI.** 1999. A sampling of the yeast proteome. Mol. Cell. Biol. **19**:7357–7368.
52. **Gygi SP, Rochon Y, Franza BR, Aebersold R.** 1999. Correlation between protein and mRNA abundance in yeast. Mol. Cell. Biol. **19**:1720–1730.
53. **de Nobel H, et al.** 2001. Parallel and comparative analysis of the proteome and transcriptome of sorbic acid-stressed *Saccharomyces cerevisiae*. Yeast **18**:1413–1428.
54. **Yin Z, et al.** 2004. Proteomic response to amino acid starvation in *Candida albicans* and *Saccharomyces cerevisiae*. Proteomics **4**:2425–2436.
55. **Leach MD, Stead DA, Argo E, MacCallum DM, Brown AJ.** 2011. Molecular and proteomic analyses highlight the importance of ubiquitination for the stress resistance, metabolic adaptation, morphogenetic regulation and virulence of *Candida albicans*. Mol. Microbiol. **79**:1574–1593.
56. **Radivojac P, et al.** 2010. Identification, analysis, and prediction of protein ubiquitination sites. Proteins **78**:365–380.
57. **Fradin C, et al.** 2005. Granulocytes govern the transcriptional response, morphology and proliferation of *Candida albicans* in human blood. Mol. Microbiol. **56**:397–415.
58. **Kusch H, et al.** 2008. A proteomic view of *Candida albicans* yeast cell metabolism in exponential and stationary growth phases. Int. J. Med. Microbiol. **298**:291–318.
59. **Leng P, Sudbery PE, Brown AJ.** 2000. Rad6p represses yeast-hypha morphogenesis in the human fungal pathogen *Candida albicans*. Mol. Microbiol. **35**:1264–1275.
60. **Roig P, Gozalbo D.** 2003. Depletion of polyubiquitin encoded by the UBI4 gene confers pleiotropic phenotype to *Candida albicans* cells. Fungal Genet. Biol. **39**:70–81.
61. **Atir-Lande A, Gildor T, Kornitzer D.** 2005. Role for the SCFCDC4 ubiquitin ligase in *Candida albicans* morphogenesis. Mol. Biol. Cell **16**: 2772–2785.
62. **Li WJ, et al.** 2006. The F-box protein Grr1 regulates the stability of Ccn1, Cln3 and Hof1 and cell morphogenesis in *Candida albicans*. Mol. Microbiol. **62**:212–226.
63. **Trunk K, et al.** 2009. Depletion of the cullin Cdc53p induces morphogenetic changes in *Candida albicans*. Eukaryot. Cell **8**:756–767.
64. **Leach MD, Brown AJ.** 2012. Posttranslational modifications of proteins in the pathobiology of medically relevant fungi. Eukaryot. Cell **11**:98–108.
65. **Roig P, Martínez JP, Gil ML, Gozalbo D.** 2000. Molecular cloning and characterization of the *Candida albicans UBI3* gene coding for a ubiquitin-hybrid protein. Yeast **16**:1413–1419.
66. **Nantel A, et al.** 2002. Transcription profiling of *Candida albicans* cells undergoing the yeast-to-hyphal transition. Mol. Biol. Cell **13**:3452–3465.
67. **Enjalbert B, Nantel A, Whiteway M.** 2003. Stress-induced gene expression in *Candida albicans*: absence of a general stress response. Mol. Biol. Cell **14**:1460–1467.
68. **Tsong AE, Miller MG, Raisner RM, Johnson AD.** 2003. Evolution of a combinatorial transcriptional circuit: a case study in yeasts. Cell **115**: 389–399.
69. **Yin Z, et al.** 2009. A proteomic analysis of the salt, cadmium and peroxide stress responses in *Candida albicans* and the role of the Hog1 stress-activated MAPK in regulating the stress-induced proteome. Proteomics **9**:4686–4703.
70. **Thewes S, et al.** 2007. *In vivo* and *ex vivo* comparative transcriptional profiling of invasive and non-invasive *Candida albicans* isolates identifies genes associated with tissue invasion. Mol. Microbiol. **63**:1606–1628.
71. **Sherman F.** 1991. Getting started with yeast. Methods Enzymol. **194**:3–21.
72. **Janke C, et al.** 2004. A versatile toolbox for PCR-based tagging of yeast genes: new fluorescent proteins, more markers and promoter substitution cassettes. Yeast **21**:947–962.
73. **Knop M, et al.** 1999. Epitope tagging of yeast genes using a PCR-based strategy: more tags and improved practical routines. Yeast **15**:963–972.
74. **Walker LA, et al.** 2009. Genome-wide analysis of *Candida albicans* gene expression patterns during infection of the mammalian kidney. Fungal Genet. Biol. **46**:210–219.
75. **Cline MS, et al.** 2007. Integration of biological networks and gene expression data using cytoscape. Nat. Protoc. **2**:2366–2382.
76. **Smith DA, Nicholls S, Morgan BA, Brown AJ, Quinn J.** 2004. A conserved stress-activated protein kinase regulates a core stress response in the human pathogen *Candida albicans*. Mol. Biol. Cell **15**:4179–4190.
77. **Enjalbert B, et al.** 2006. Role of the Hog1 stress-activated protein kinase in the global transcriptional response to stress in the fungal pathogen *Candida albicans*. Mol. Biol. Cell **17**:1018–1032.
78. **Enjalbert B, MacCallum DM, Odds FC, Brown AJ.** 2007. Niche-specific activation of the oxidative stress response by the pathogenic fungus *Candida albicans*. Infect. Immun. **75**:2143–2151.
79. **Imbeaud S, Auffray C.** 2005. Functional annotation: extracting functional and regulatory order from microarrays. Mol. Syst. Biol. **1**:.0009.